

# ON THE WEAKENING OF CHROMOSPHERIC MAGNETIC FIELD IN ACTIVE REGIONS

K. Nagaraju

*Indian Institute of Astrophysics, Koramangala, Bangalore-560034, India;  
nagaraj@iiap.res.in*

K. Sankarasubramanian

*ISRO Satellite Center, Airport road, Monera, Bangalore-560017, India;  
sankark@isac.gov.in*

and

K. E. Rangarajan

*Indian Institute of Astrophysics, Koramangala, Bangalore-560034, India;  
rangaraj@iiap.res.in*

## ABSTRACT

Simultaneous measurement of line-of-sight (LOS) magnetic and velocity fields at the photosphere and chromosphere are presented. Fe I line at  $\lambda 6569$  and  $H_\alpha$  at  $\lambda 6563$  are used respectively for deriving the physical parameters at photospheric and chromospheric heights. The LOS magnetic field obtained through the center-of-gravity method show a linear relation between photospheric and chromospheric field for field strengths less than 700 G. But in strong field regions, the LOS magnetic field values derived from  $H_\alpha$  are much weaker than what one gets from the linear relationship and also from those expected from the extrapolation of the photospheric magnetic field. We discuss in detail the properties of magnetic field observed in  $H_\alpha$  from the point of view of observed velocity gradients. The bisector analysis of  $H_\alpha$  Stokes  $I$  profiles show larger velocity gradients in those places where strong photospheric magnetic fields are observed. These observations may support the view that the stronger fields diverge faster with height compared to weaker fields.

*Subject headings:* Sun: magnetic fields - Sun: photosphere - Sun: chromosphere - sunspots

## 1. INTRODUCTION

It is inferred through various observations that the magnetic field is playing a central role in the solar energetics that take place in the higher layers of the atmosphere (see for eg. Regnier & Canfield (2006)). But, it is somewhat difficult to obtain a reliable vector magnetic field measurements at the chromosphere and corona (Socas-Navarro 2005; Judge 2007). The measurements of the photospheric magnetic fields are relatively well established. However, simultaneous vector magnetic field observations at the photospheric and chromospheric heights will give a better handle on the understanding of the magnetic structuring of the solar atmosphere. More direct and reliable measurements of the magnetic field at the chromosphere will also serve as a better boundary condition for extrapolating the magnetic fields to the coronal heights.

Measurements of the vector magnetic field in  $H_\alpha$  is particularly important in understanding the connection between photospheric, chromospheric and coronal magnetic field as its height of formation ranges almost from the upper photosphere to upper chromosphere (Vernazza et al. 1981). Also, this is one of the most widely used spectral lines for the study of solar chromosphere (see a recent review by Rutten (2007)).

Comparison of the active region magnetic fields measured in  $H_\alpha$  and in the photosphere show a one-to-one correspondence in the weak field regions. But in the strong field regions, like umbra, there is a considerable deviation from the linearity (Balasubramaniam et al. 2004; Hanaoka 2005). Infact the LOS magnetic field measured in  $H_\alpha$  weakens much faster for the corresponding strong field regions of the photosphere. At this point it may not be appropriate to demarcate the field strength above which this deviation happens because different observations show different deviation points. Gosain & Choudhary (2003) have also reported the systematic weakening of the magnetic field derived from Mg I  $\lambda 5173/5184$  lines in comparison with that of Fe I  $\lambda 6301.5/6302.5$  lines. In their case, the magnetic field measured by Mg I lines agree with the potential field extrapolation of the photospheric LOS magnetic field in weak field regime. In strong field regions there is a systematic shift towards lower values but still linear. Simultaneous observations of He I at  $\lambda 10830$  and Si I lines at  $\lambda 10827.1$  by Choudhary et al. (2002) suggest that the field diverges faster in the upper layers of the chromosphere.

However there is no conclusive explanation for the observed weaker chromospheric magnetic fields for the corresponding strong photospheric fields. Various possibilities have been discussed by Balasubramaniam et al. (2004) & Hanaoka (2005) about weaker chromospheric fields observed in umbra. Hanaoka (2005) have discussed the possibility of scattered light and/or peculiarity of the atmosphere (radiative transfer effects) for the decrease in the polarization signal which in turn cause the underestimation of the magnetic field.

Balasubramaniam et al. (2004) have suggested that the strongest fields measured at the photosphere diverge spatially and more quickly than the weak fields when propagating upward. In this paper, we address these issues from the point of view of the observed velocity gradients.

It is well known that, velocities and magnetic fields are coupled to each other in the solar atmosphere (see for eg. Rajaguru et al. (2006)). Any change in the magnetic field is expected to alter the plasma motion and hence the observed velocity. If the field strength decreases with height then the velocity is expected to increase and vice versa, for the simple reason that the inhibition of the plasma depends on the magnetic field strength (Spruit & Zweibel 1979). It is also well known that the magnetic field strength in the umbral region at the photosphere is large. If the magnetic field measured with  $H_\alpha$  in the umbral region is weaker, then it shows that the magnetic field gradient is larger than expected which implies larger velocity gradients in the umbral region compared to the penumbral region at chromospheric heights. In order to observationally verify this we have analyzed the velocity and magnetic fields estimated from the simultaneous spectropolarimetric observations of an active region using  $H_\alpha$  and Fe I spectral lines.

The spectropolarimetric observations which were carried out at the Kodaikanal solar telescope using a dual beam polarimeter are discussed in section(2). Sections (3) and (4) discuss the data reduction and analysis procedures respectively. A comparison of LOS magnetic field at the chromosphere and photosphere is presented in section (5.1). Velocity gradients obtained through bisector technique are discussed in section (5.2).

## 2. INSTRUMENT AND OBSERVATIONS

Spectropolarimetric observations were carried out using a newly added dual beam polarimeter to the spectrograph at Kodaikanal solar telescope (Nagaraju et al. (2007) and also see Bappu (1967) for details about the spectrograph and telescope setup). The wavelength region of the observations presented in this paper includes  $H_\alpha$  ( $\lambda 6563$ ) and Fe I ( $\lambda 6569$ ) lines. Both  $H_\alpha$  and Fe I lines are magnetically sensitive with effective Landé 'g' factor of 1.048 (Casini & Landi Degl'Innocenti 1994) and 1.4 (Kobanov et al. 2003) respectively. The measured instrumental broadening and the linear dispersion close to this wavelength region in second order of diffraction are  $38 \pm 0.5 m\text{\AA}$  and  $10.15 m\text{\AA}/pixel$  respectively. The wavelength calibration was done using the telluric lines ( $H_2O$ ) at  $\lambda 6570.63$  and  $\lambda 6561.097$  (Moore et al. 1966).

An eight stage modulation scheme was used for the measurement of the general state

of polarization (Nagaraju et al. 2007). In this modulation scheme the measurement of the Stokes parameters are well balanced over the duration of eight stages of intensity measurements. The rotation of the retarders were done manually for the modulation of the input light.

The spectropolarimetric data of an active region NOAA0875 presented in this paper were obtained on 28th April, 2006. The heliographic coordinates of the sunspot during observations were  $11^\circ$  south and  $18^\circ$  west. Scanning of the sunspot was done by moving the Sun’s image in an east-west direction in steps of  $\approx 5''$ . For each slit position, the modulated intensities were recorded by the CCD detector. The CCD is a  $1K \times 1K$  Photometrics detector with the pixel size of  $24\mu$ . Eight stages of modulation took about 90 s with a typical exposure time of 0.5 s.

### 3. DATA REDUCTION

The spectral images were corrected for dark current and gain table variation of the pixels (details about the flat fielding of spectropolarimetric data can be found in Schlichenmaier & Collados (2002); Beck et al. (2005)).

Model independent velocity and magnetic field gradients can be derived from the bisector technique for the range of heights over which the spectral line is formed, provided the full spectral profile is available without any blend (Balasubramaniam et al. 1997; Sankarasubramanian & Rimm 2002). The application of bisector technique to  $H_\alpha$  is restricted because of the blend in its red wing by the Zeeman sensitive Co I ( $\lambda 6563.4$ ) line which forms at the photospheric heights. In the following section we discuss the procedure to remove this blend and its limitations.

#### 3.1. Blend Removal Procedure

Individual profiles of  $H_\alpha$  corresponding to the orthogonally polarized beams in each stage of modulation were considered for removing the blend. A function which is a linear combination of a Gaussian and a quadratic term was fitted to the blend region of the observed  $H_\alpha$  profile. This non-linear least square fit (available in IDL) takes into account the curvature in the intensity profile of  $H_\alpha$  line along with the Co I line profile approximated as a Gaussian. The Gaussian, constructed out of the fitted parameters, was removed from the observed profile. Then the eight intensity measurements were combined to obtain Stokes  $I$ ,  $Q$ ,  $U$  and  $V$  spectral images through the demodulation procedure explained in Nagaraju et al. (2007). A typical  $H_\alpha$  intensity profile before and after the blend removal is shown in Fig. 1 with the

bisectors marked as diamond symbols.

Even though it appears in the total intensity profile that the effect of Co I line is completely removed, the blend residuals still appear in Stokes  $Q$ ,  $U$ , and  $V$  profiles. The residuals are due to the Gaussian approximation used for the Co I line profile. However, it is demonstrated in the section 5.2 that the blend residuals do not have any effect on the velocity gradients calculated from the  $H_\alpha$  intensity profiles.

The better way to remove the blend may be to synthesise the Stokes profiles of Co I using radiative transfer equations along with the atmospheric parameters obtained through Fe I ( $\lambda 6569$ ) line. However in this paper only Stokes  $I$  profiles are considered for the velocity gradients estimation and a restricted spectral range of  $H_\alpha$  about line center for the LOS magnetic field estimation. Hence, the simple blend removal method outlined in this paper is found to be sufficient.

### 3.2. Correction for Polarimeter Response and Telescope Induced Cross-talks

The polarimetric data was corrected for polarimeter response (for details see Nagaraju et al. (2007)). The instrumental polarization introduced by the telescope was corrected by using the telescope model developed by Balasubramaniam et al. (1985) and Sankarasubramanian (2000). The refractive index values for Aluminium coating used in the model are obtained from the catalog (Walter 1978). Since these values may be different from the actual values, there still remain residual cross-talks among Stokes parameters. These residual cross-talks are removed by the statistical method given in Schlichenmaier & Collados (2002).

## 4. DATA ANALYSIS

### 4.1. LOS Magnetic Field

The LOS magnetic fields at the photospheric and chromospheric heights are derived using the Fe I line and  $H_\alpha$  respectively. For the derivation of the LOS magnetic fields, center-of-gravity (COG) method was used (Rees & Semel 1979; Cauzzi et al. 1993; Uitenbroek 2003; Balasubramaniam et al. 2004).

For the COG method, the LOS field strength is given by

$$B_{LOS} = \frac{(\lambda_+ - \lambda_-)/2}{4.667 \times 10^{-13} \lambda_0^2 g_L}, \quad (1)$$

where  $\lambda_0$  is the central wavelength of the line in  $\text{\AA}$ ,  $g_L$  is the Landé ‘g’ factor of the line, and  $\lambda_{\pm}$  are the COG wavelengths of the positive and negative circularly polarized components respectively. The COG components are calculated as

$$\lambda_{\pm} = \frac{\int [I_{cont} - (I \pm V)] \lambda d\lambda}{\int I_{cont} - (I \pm V) d\lambda} \quad (2)$$

where  $I_{cont}$  is the local continuum intensity. The integration is over the spectral range of a given spectral line. Since Fe I line is free of blend, the full spectral range is available for the COG method. For the  $H_{\alpha}$  line, the spectral range is restricted due to the blending of the Zeeman sensitive Co I line. Even though the blend is removed in Stokes  $I$  profile using the Gaussian fit technique explained in the section (3.1), there still remains a residual in polarization profiles. To avoid introducing any artifacts in the LOS magnetic field values derived using COG method, a restricted spectral range about the  $H_{\alpha}$  line core is used. This spectral region was selected by looking at the strongest Stokes  $V$  signal of Co I line. Hence the derived LOS magnetic field using  $H_{\alpha}$  would correspond mostly to the upper chromosphere (Rutten 2007).

The expected maximum underestimation of the photospheric LOS magnetic field is about 12% for the kind of field strengths presented in this paper. Because of the large intrinsic Doppler width of  $H_{\alpha}$ , the underestimation of the LOS field is not expected even for the strongest magnetic field observed at the chromosphere (Uitenbroek 2003). However we checked the reliability of the COG method in deriving LOS field from  $H_{\alpha}$  by applying it to synthetic Stokes  $I$  and  $V$  profiles of  $H_{\alpha}$  obtained using the radiative transfer code of Uitenbroek (1998). From these studies it was found that the COG method overestimates the LOS field by about 1.5% in the field strength range 0 to 2000 G. However, the main error involved in the determination of the LOS magnetic field, for this observation, is due to the error in estimating the shifts between the COG wavelength positions  $\lambda_+$  and  $\lambda_-$  which is expected to be less than 70 G.

## 4.2. Photospheric Vector Magnetic Field

The strength and the orientation of the chromospheric magnetic field are very much dependent on its vector nature at the photosphere (Wiegmann et al. (2006) and references there in). Inference of the vector magnetic field at the chromosphere from the  $H_{\alpha}$  observations is difficult because, Stokes  $Q$  and  $U$  are hardly discernible. Only at few locations of penumbra they are above the noise level ( $2 \times 10^{-3} I_{cont}$  in our observations). Hence for the correct interpretation of the LOS magnetic field obtained from  $H_{\alpha}$  it is important to have

the complete information about the vector magnetic field at the photosphere.

The photospheric vector magnetic fields are obtained by inverting the observed Stokes profiles of Fe I line. Milne-Eddington Line Analysis using a Numerical Inversion Engine (MELANIE)<sup>1</sup> was used to perform the inversion. MELANIE performs non-linear least-square fitting of the observed Stokes profiles under Local-Thermodynamic-Equilibrium (LTE) condition by assuming Milne-Eddington atmosphere. Inversion code returns magnetic field strength, inclination angle with respect to LOS, azimuth, line strength, damping parameter, LOS velocity, source function and its gradient with optical depth, macroturbulence and fraction of stray light/fill factor of the non-magnetic component.

The fit error in estimating the magnetic field ranges from 50 G for the Stokes profiles which are symmetric and well above the noise level to 250 G for the Stokes profiles which are highly asymmetric and close to noise level. The maximum fit error in the estimation of the field orientation is about 5° and its azimuth is 6°. Other physical parameters returned by the MELANIE are not used in the current work and hence are not discussed here.

### 4.3. Velocity Gradients

The measurement of the magnetic field in  $H_\alpha$  has been difficult to interpret (Balasubramaniam et al. 2004; Hanaoka 2005). However it is possible to address some of these difficulties from the study of plasma motions as magnetic field and plasma motion influence one another in the solar atmosphere (Gary 2001). Hence the study of velocity and its gradient may help in better interpretation of the observed magnetic field.

The velocities at the photosphere and chromosphere are obtained through COG method (Uitenbroek 2003). The COG wavelength  $\lambda_{COG}$  of a line profile  $I$  is defined as the centroid of its residual intensity profile:

$$\lambda_{COG} = \frac{\int \lambda(I_{cont} - I)d\lambda}{\int (I_{cont} - I)d\lambda}. \quad (3)$$

The LOS velocity with respect to the average quiet Sun reference ( $\lambda_{ref}$ ) is defined as

$$v_{LOS} = \frac{c(\lambda_{COG} - \lambda_{ref})}{\lambda_{ref}}, \quad (4)$$

where  $c$  is the speed of the light.

---

<sup>1</sup><http://www.hao.ucar.edu/public/research/cic/index.html>

Bisector technique has been applied to Stokes  $I$  profiles to derive the velocity gradients both at the photosphere and chromosphere. The Stokes  $I$  profiles of Fe I and  $H_\alpha$  are separately considered for bisector analysis. Bisectors are obtained at 9 equal intensity levels between line core and the wing for Fe I and 14 equal intensity levels between line core and wing for  $H_\alpha$  respectively. Out of 9 bisectors of Fe I line only 7 are considered, namely, the bisectors between second and eighth counting from the line core. Similarly for  $H_\alpha$  the bisectors between second and thirteenth are considered totalling 12 bisectors. The bisectors very close to line core and wing are not considered because of the lower signal-to-noise ratio and to avoid the influence of the continuum respectively. For the Fe I line, the wavelength position of the second bisector which corresponds to higher atmospheric layer was subtracted from the seventh bisector which corresponds to lower atmospheric layer. Similarly for  $H_\alpha$ , the wavelength position of the second bisector was subtracted from the thirteenth bisector. The wavelength differences ( $\Delta\lambda$ s) thus obtained are converted into velocities - which would then represent the velocity difference between the lower and higher atmospheric layers - using the following relation,

$$\Delta V_{bs} = \frac{c\Delta\lambda}{\lambda_0}. \quad (5)$$

Where  $\lambda_0$  is the rest wavelength of the spectral line under consideration. The velocity difference defined in Eq. (5) represents the velocity gradient over the line formation height.

The errors in estimating the velocity differences are mainly due to the errors involved in finding the wavelength shifts. The maximum error in estimating the velocity gradients is about  $0.09 \text{ km s}^{-1}$ .

#### 4.4. Stokes $V$ Amplitude Asymmetry

Amplitude and area asymmetries of Stokes  $V$  profiles are caused by the gradients in the velocity and magnetic fields (see for eg. Sanchez Almeida & Lites (1992); Sankarasubramanian & Rimmele (2002)). Hence their analysis will give us some handle on the understanding of the field gradients.

If  $a_r$  and  $a_b$  represent the amplitudes of red and blue wings of Stokes  $V$  respectively then the amplitude asymmetry is defined as,

$$\delta a = \frac{|a_b| - |a_r|}{|a_b| + |a_r|}. \quad (6)$$

The area asymmetry is not considered in this paper due to the difficulty in estimating it for the  $H_\alpha$  in the presence of Co I line blend.

## 5. RESULTS AND DISCUSSIONS

### 5.1. Comparison of Photospheric and Chromospheric LOS Magnetic Fields

The scatter plot of LOS magnetic field derived from  $H_\alpha$  and Fe I is shown in Fig. 2. The plot shows that the chromospheric magnetic field is weaker in general compared to its photospheric counterpart. The important point to note from this figure is that the chromospheric fields are much weaker in the locations where the strong photospheric fields are observed. Similar kind of observations were reported earlier by Balasubramaniam et al. (2004) using simultaneous observations in  $H_\alpha$  and Fe I line at  $\lambda 6301.5$  and Hanaoka (2005) who compared the LOS field measured in  $H_\alpha$  with the magnetograms of SOHO/MDI. These observations may imply that the stronger fields weaken much faster when they propagate upward in the solar atmosphere.

To illustrate the quicker weakening of the stronger fields, plots of the photospheric and the chromospheric LOS field strengths along two different radial slices of the sunspot are shown on the right side of the Fig. 3. The radial slices considered for this purpose are marked as 1 and 2 on the SOHO/MDI intensitygram showing the sunspot analysed in this paper <sup>2</sup>. The top panel on the right side of the Fig. 3 shows the plots of photospheric and chromospheric LOS magnetic field strengths along the radial cut (marked as 1 on the sunspot image) passing close to the central umbra. Note that, along this radial cut the photospheric field strength increases systematically from the penumbral region to the umbral region. While the chromospheric field strength increases upto about 800 G, more or less linear with the photospheric field, and then starts decreasing towards the umbra. The decrease in the chromospheric field is much larger close to central umbra. The photospheric field along the radial cut 2 as shown in the bottom panel on the right side of the Fig. 3 shows the behavior very similar to that was seen along the radial cut 1. That means the photospheric field strength is larger in the umbral region and decreases towards the edges of the sunspot. In the case of chromospheric field strength, the values do not decrease towards the umbra as was seen for the radial cut 1 but, they are considerably smaller compared to its photospheric counterpart. The main difference between these two radial cuts is that the field strength in the umbral photosphere for radial cut 1 is larger compared to that of radial cut 2. This may be an indication of the faster divergence of the stronger fields. However, there are other possibilities which can cause this observed weaker fields in the umbral chromosphere and

---

<sup>2</sup>Because of the coarser step size used for scanning the sunspot ( $\approx 5$  arc sec), the raster images do not give a good representation of the observed region and also there was no imaging facility available during these observations and therefore intensitygram from SOHO/MDI is used. The radial cuts marked on the image represent the approximate slit positions of the observations.

they are : weakening of the polarization signal due to scattered light within the instrument and from nearby quiet Sun; peculiarity of the atmosphere such as discussed by Hanaoka (2005); the methods used to derive LOS magnetic field (inversion of  $H_\alpha$  Stokes profiles is yet to be established); inclination of the magnetic field; and most importantly the height of formation which is highly ambiguous (Socas-Navarro & Uitenbroek 2004). We will discuss these issues in detail after looking at the results from the analysis of velocity gradients both at the photosphere and chromosphere.

## 5.2. Velocity Gradients and the Nature of the Magnetic Fields

The velocities calculated using COG method show a typical behavior of Evershed flows both at the photosphere and chromosphere. That means the limb side penumbra shows red shift with respect to quiet Sun where as center side penumbra shows blue shift at the photospheric heights. The situation is exactly opposite at chromospheric heights which are consistent with the well known inverse Evershed effect. COG velocities in umbral regions both at photosphere and chromosphere are smaller compared to penumbral regions.

The plots of bisector velocity differences (Eq. 5) as a function of photospheric magnetic field strength are shown in Fig. 4 for the Fe I line. Top panel in this figure is for all the points over the total field of view (FOV), where as the bottom left and right panel is for umbral and penumbral regions of the observed spot, respectively. Note from these figures that the large number of points correspond to umbra have smaller velocity gradients than the penumbra. Closer investigation of bisector velocity differences of Fe I line show the flow pattern consistent with the well known Evershed flow. That means larger portion of the limb side penumbra shows net downflow (both core and wing side bisectors show redshifts) and disk center side penumbra shows net upflow (both core and wing bisectors show blue shifts with respect to the reference). For the definition of the net up- and down-flow see Balasubramaniam et al. (1997).

We also found that the bisector velocity gradients and COG velocities observed in Fe I show a good correlation in agreement with the earlier observations. That means, larger the COG velocity larger the velocity gradient at the photosphere.

In Fig. 5 the plots of bisector velocity gradients for  $H_\alpha$  v/s the photospheric magnetic fields are shown. Top panel in this figure is for the total FOV and left bottom panel for umbral region and right bottom panel for penumbral region. Notice the increase in bisector velocity gradients measured in  $H_\alpha$  with increase in the photospheric magnetic field strength. Plots of velocity gradients along two radial slices of sunspot (marked as 1 and 2 in Fig.

3) also show that the larger velocity gradients at the chromosphere are located at which strong photospheric fields are observed (Fig. 6). Top panels in Fig. 6 show the plots of photospheric field strengths along the radial cut 1 and the radial cut 2. The corresponding plots of velocity gradients are shown in the bottom panels. Except at few locations (mostly in the limb side penumbra such as shown in the bottom right panel of Fig. 6) which show less variation in the values of velocity gradients inspite of variation in the photospheric field strengths (which is evident also in Fig. 5), most of the places the velocity gradients are larger where the photospheric magnetic field strengths are larger.

Closer examination of the bisector wavelength positions of  $H_\alpha$  Stokes  $I$  profiles in different regions of the sunspot with respect to the reference wavelength reveals the following results (see figure 7).

- In the limb side penumbra both line core and wing side bisectors show blue shift with respect to quiet Sun. The shifts in the line core bisectors are large compared to the line wing bisectors indicating the net upflow.
- In the umbral region also both line core side and wing side bisectors show blue shifts with respect to the reference wavelength. The shifts in the line core side bisectors for the umbra are almost comparable to that of the limb side penumbra. However, the shifts in the line wing side bisectors for the umbra are much smaller with respect to that of the limb side penumbra. This would indicate again the net upflows but with larger velocity gradients.
- In the center side penumbra the line wing bisectors show redshift in most of the places with respect to the quiet Sun. At few locations they show a small blue shift or no shift. The line core side bisectors show slight blue shift with respect to quiet Sun reference wavelength position.

It is found through these analyses that the velocity gradients are larger in the umbra at the chromospheric heights compared to the penumbra (see Fig. 5). Which is exactly in contrast with the flow pattern observed at the photosphere. The analysis of bisector velocity differences also indicate accelerated upflows in the umbral region.

There is a little concern due to the residuals present after the Co I line blend is removed. To make sure that there are no artifacts introduced due to the residuals, the bisector velocity differences calculated by considering the spectral region of the line which is not affected by the blend are shown in Fig. 8 as a function of photospheric field strength. This figure also shows the trend that the velocity gradients increase with increase in photospheric magnetic

field strength confirming the observations made with the blend removed full intensity profiles. As expected, the gradients are smaller due to the smaller wavelength regions considered in this case.

To summarise, wavelength shifts analysis of Stokes  $I$  bisectors show that the velocity gradients are larger in the umbral region than in the penumbral region at the chromospheric heights. Most importantly, accelerated upflows are observed in the umbral region. In other words, LOS velocity increases upward more rapidly in the umbral region than in the penumbral region at the chromosphere.

Let us now address some of the possibilities, mentioned in the beginning of this section, which can cause the observed weaker chromospheric field in the umbral region from the point of view of the velocity gradients.

We found that the stray light within the instrument is less than 2% by comparing the quiet Sun spectrum with the atlas (Wallace et al. 2000). This amount of stray light is too small to account for the observed weaker Stokes  $V$  signals in the umbral region. Also, it can not account for the observed velocity gradients in  $H_\alpha$ .

The next question raised was about the reliability of the methods used to estimate the LOS magnetic field. Despite the availability of more accurate estimation of photospheric magnetic field through inversion, we have used the COG method to maintain the uniformity while comparing the LOS field at the photosphere and chromosphere (Fig. 2). This is because the inversion of  $H_\alpha$  profiles to derive magnetic field is yet to be established. As discussed in section 4.1 the underestimation of the LOS field obtained from Fe I is expected to be more while the values obtained from  $H_\alpha$  will be less as confirmed through numerical simulations. Also, the observed umbral fields are larger at the photosphere where as they are smaller at the chromosphere. Hence the departure of LOS magnetic fields from the actual values due to the method used to estimate them can not explain the observed weakening of the magnetic fields.

One of the possibilities which can cause the reduction in polarization (in effect the weaker magnetic field) proposed by Hanaoka (2005) is the peculiarity of the atmosphere. However, the kind of peculiarity discussed by him can not explain the velocity gradients and the Stokes profiles of  $H_\alpha$  discussed in this paper.

It is a general wisdom gained from the extrapolation technique that the magnetic topology at the chromosphere is very much dependent on the field configuration at the photosphere. Extrapolation techniques like potential field approximation suggest that larger the field inclination at the photosphere chromospheric fields should also show larger inclination. From the inversion of Fe I line it was found that the fields are oriented more close to LOS

in the umbral region than in the penumbral region. Hence we expect larger field orientation in penumbral region at the chromospheric heights also. As mentioned in section 4.2  $H_\alpha$  shows Stokes  $Q$  and  $U$  signals which are above the noise level in penumbral region but not in umbral region indicating that the orientation of the fields are larger in the penumbral region compared to the umbral region even at the chromosphere. Hence we believe that the weaker LOS field observed in the umbral region may not be due to the larger orientation angle with respect to the LOS. This scenario is also verified using the velocity gradients observed at the chromosphere, as larger inclination means smaller LOS velocity in contradiction to the observed velocities (Fig. 5).

Another major difficulty in interpreting the  $H_\alpha$  observations is the ambiguity in its height of formation. Studies based on the response functions by Socas-Navarro & Uitenbroek (2004) show that the  $H_\alpha$  is sensitive mostly to chromospheric magnetic field in the umbral model. While in the quiet Sun model it shows sensitivity to both photospheric and chromospheric magnetic fields. Since the magnetic fields at the photosphere is large, the magnetic field measured in quiet Sun regions will mostly be photopsheric. If the  $H_\alpha$  were to show the sensitivity to magnetic field in the penumbral model similar to that of quiet Sun model then one would expect larger field values in the penumbra which will be an average of photospheric and chromospheric fields while the umbral fields are exclusively chromospheric. To confirm this, more forward modeling is needed which includes the comparison of  $H_\alpha$  line formation at different regions with different field configurations. More over, response of  $H_\alpha$  line to various physical parameters needs to be studied and consistently explain the observations such as velocity and velocity gradients presented in this paper.

Other possibility which can cause the observed weaker chromospheric fields in the umbral region is the faster divergence of stronger fields as suggested by Balasubramaniam et al. (2004). This scenario may consistently explain both the observed magnetic properties (Fig. 2 ) as well as the velocity properties (Figs. 5/8). Because of the decrease in the field strength, the plasma becomes less inhibited by the magnetic fields and hence more free to move. That means if the stronger fields diverge faster compared to weaker fields then the the velocities should increase faster in the stronger field regions which are consistent with the observations.

### 5.3. Stokes $V$ Amplitude Asymmetry

From the close examination of Stokes  $V$  profiles of  $H_\alpha$  we found that the Co I line has not intruded up to the extent that the amplitudes are affected. Hence the results presented from  $H_\alpha$  based on amplitude asymmetry are reliable.

From the Fig. 9 it is clear that the amplitude asymmetry of Fe I line tends toward zero with increase in photospheric magnetic field strength. This means, at the photospheric heights the gradients are smaller in umbra which corresponds to the region of strong fields. In contrast amplitude asymmetry observed in  $H_\alpha$  tend to increase with photospheric field strength as shown in the Fig. 10. This implies that the field gradients are larger in the umbra at the chromosphere compared to penumbra. Hence the analysis of amplitude asymmetry confirm the results obtained from the bisector analysis in section 5.2.

## 6. CONCLUSIONS

In this paper we have used the multiwavelength spectropolarimetric tool to understand the stratification of the magnetic and velocity fields in the solar atmosphere. Out of the two lines considered for spectropolarimetry, one forms at photospheric height (Fe I  $\lambda 6569$ ) and the other spans almost from the upper photosphere to upper chromosphere ( $H_\alpha$ ). Hence, these lines were useful in studying the connection between physical parameters at the photospheric and chromospheric heights. The main physical parameters studied in this paper are the magnetic and velocity fields in an active region.

As discussed in section 5.1, the LOS magnetic field measured in chromosphere is in general weak compared to its photospheric counterpart. The weakening of the chromospheric field is much faster for the corresponding strong photospheric field. The magnetic field strengths observed in the umbral chromosphere are much weaker than those expected from the extrapolation of the photospheric magnetic field. For instance, the field strength inferred through  $H_\alpha$  observations is about 400 G where as the field strength obtained through the extrapolation of the observed photospheric field under potential field approximation to an height of 2000 km is about 1000 G (assuming that the height of formation of  $H_\alpha$  is about 2000 km). Various possibilities have been discussed which can cause the weaker fields observed in the umbral chromosphere. The most probable ones are the fast divergence of the stronger fields when they propagate upward in the atmosphere (Balasubramaniam et al. 2004) and ambiguity in the height resolution of  $H_\alpha$  magnetic sensitivity which may be photospheric and/or chromospheric depending on the region of observation (Socas-Navarro & Uitenbroek 2004). If former is the reason, then it can explain the observed properties of both velocity and the magnetic fields presented in this paper. This is because, as shown in Fig. 3, observed chromospheric fields are systematically weaker at the locations where strong photospheric fields are observed. If the weaker field strengths observed at the umbral chromosphere are truly of solar origin then this implies that the umbral fields decrease more rapidly with height compared to penumbral fields. Rapid decrease in field strengths cause rapid increase

in velocity with height as there is a small upflow in the umbral photosphere. Observations also show that the velocity increases more rapidly in the umbral region compared to penumbral region (section 5.2). Earlier observations by Gosain & Choudhary (2003) have also indicated the weakening of the magnetic field which is larger for stronger fields. In their observations quicker weakening of the stronger fields is not apparent, probably, because of the lines (Mg I b1 and b2 at  $\lambda 5173$  and  $\lambda 5184$ ) used to infer chromospheric magnetic field that originate at the lower chromosphere. While the observations based on  $H_\alpha$  presented in this paper as well as earlier by Balasubramaniam et al. (2004); Hanaoka (2005) show clearly that the strong fields weaken quickly with height because in these works, to infer chromospheric magnetic field only the spectral region close to its line core is considered which samples mostly the higher layers of the chromosphere (Rutten 2007). Hence there is a possibility that the weaker LOS field strengths observed in the umbral chromosphere are caused due to the faster divergence of the stronger fields. However, we would like to caution that the reliability of the COG method in estimating the LOS magnetic field strengths discussed in this paper (section 4.1) is for simple solar atmospheric model. But, in reality the solar atmosphere may be complicated. More studies on the magnetic and velocity response functions for  $H_\alpha$  in different regions will help in better interpretation of the observations. Simultaneous multiline spectropolarimetry, which includes  $H_\alpha$  and at least one more line which is formed at the chromosphere (preferably Infrared *Ca* Triplet line at  $\lambda 8542$ ) and a photospheric line, is needed to get further insight into the physical processes that take place in the chromosphere.

Hector Socas-Navarro and Han Uitenbroek are thankfully acknowledged for providing us MELANIE and RH codes. We thank K. S. Balasubramaniam for his critical comments on our earlier version of this paper. We also thank S. P. Rajaguru for useful discussions regarding the connection between velocity and magnetic field gradients and B. Ravindra for providing us the extrapolated magnetic field strengths under potential field approximation. Thanks to the help of Devendran and Hariharan during the observations. The sunspot image was obtained from SOHO/MDI data archive. SOHO is a mission of international cooperation between ESA and NASA.

## REFERENCES

- Balasubramaniam, K. S., Christopoulou, E. B., & Uitenbroek, H. 2004, ApJ, 606, 1233
- Balasubramaniam, K. S., Keil, S. L., & Tomczyk, S. 1997, ApJ, 482, 1065
- Balasubramaniam, K. S., Venkatakrisnan, P., & Bhattacharya, J. C. 1985, Sol. Phys., 99, 333

- Bappu, M. K. V. 1967, *Sol. Phys.*, **1**, 151
- Beck, C., Schmidt, W., Kentischer, T., & Elmore, D. F., 2005, *A&A*, 437 1159
- Casini, R., & Landi Degl’Innocenti, E. 1994, *A&A*, 291, 668
- Cauzzi, G., Smaldone, L. A., Balasubramaniam, K. S., & Keil, S. L. 1993, *Sol. Phys.*, 146, 207
- Choudhary, D. P., Suemastu, Y., & Ichimoto, K. 2002, *Sol. Phys.*, 209, 349
- Gary, G. A. 2001, *Sol. Phys.*, 203, 71
- Gosain, S., & Choudhary, D. P. 2003, *Sol. Phys.*, 209, 349
- Hanaoka, Y., 2005, *Publ. Astron. Soc. Japan*, 57, 235
- Judge, P. G. 2007, *ApJ*, 662, 677
- Kobanov, N. I., Makarchik, D. V., & Sklyar, A. A. 2003, *Sol. Phys.*, 217, 53
- Moore, C. E., Minneart, M. G. J., Houtgast, J., & Rowland, H. A. 1966, *The Solar Spectrum 2935 Å to 8770 Å*. (Washington:NIST)
- Nagaraju, K., Ramesh, K. B., Sankarasubramanian, K., & Rangarajan, K. E. 2007, *Bull. Astro. Soc. India*, 35, 307
- Rajaguru, S. P., Wachter, R., & Hasan, S. S. 2006, *ILWS*, Goa
- Rees, D. E., & Semel, M. D. 1979, *A&A*, 74, 1
- Regnier, S., & Canfield, R. C. 2006, *A&A*, 451, 319
- Rutten, R. J., 2007, in *ASP Conf.Ser.368, The Physics of Chromospheric Plasmas*, ed. P. Heinzel, I. & R. J. Rutten, 27
- Sanchez Almeida, J., & Lites, B. W. 1992, *ApJ*, 398, 359
- Sankarasubramanian, K., & Rimmele, T. R. 2002, *ApJ*, 576, 1048
- Sankarasubramanian, K. 2000, *Ph.D. thesis*, Bangalore Univ.
- Schlichenmaier, R., & Collados, M. 2002, *A&A*, 381, 668
- Socas-Navarro, H. 2005, *ApJ*, 631, L67

- Socas-Navarro, H., & Uitenbroek, H. 2004, ApJ, 603, L129
- Spruit, H. C., & Zwibel, E. G. 1979, Sol. Phys., 62, 15
- Uitenbroek, H. 1998, ApJ, 498, 427
- Uitenbroek, H. 2003, ApJ, 592, 1225
- Vernazza, J. E., Avrett, E. H., & Loeser, R. 1981, ApJS, 45, 635
- Wallace, L., Hinkle, K., & Livingston, W. 2000, An atlas of sunspot umbral spectra in the visible, from 15,000 to 25,500  $cm^{-1}$  (3920 to 6664  $\text{\AA}$ )
- Walter, D. G. 1978, Hand Book of Optics, McGraw-Hill Book Company, New York
- Wiegelmann, T., Inhester, B., Kleim, B., Valori, G., & Neukirch, T. 2006, A&A, 453, 737

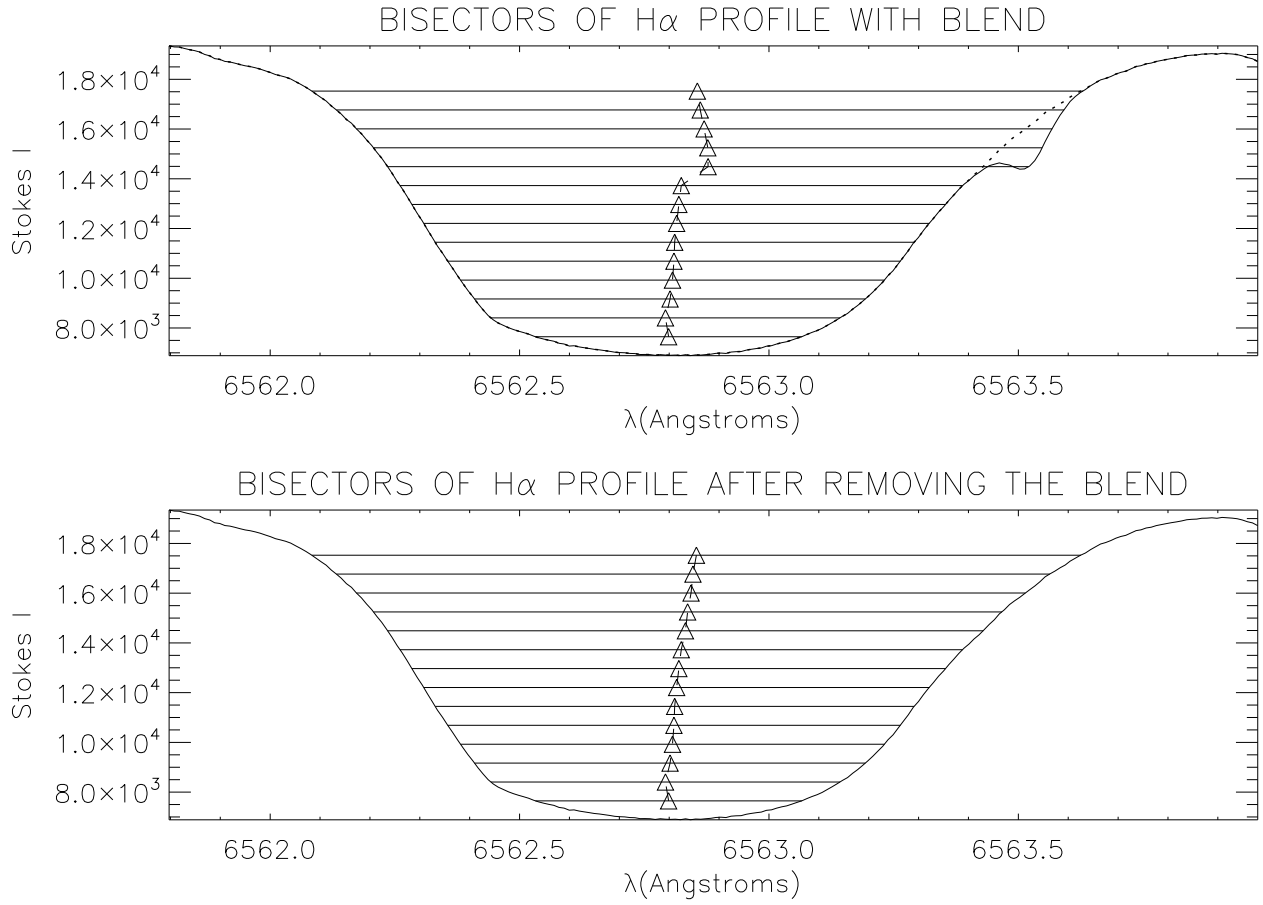


Fig. 1.— Typical  $H_\alpha$  Stokes  $I$  profile with the bisectors marked in diamond symbols. Dotted line in the top panel shows the spectral region of the profile after removing the blend.

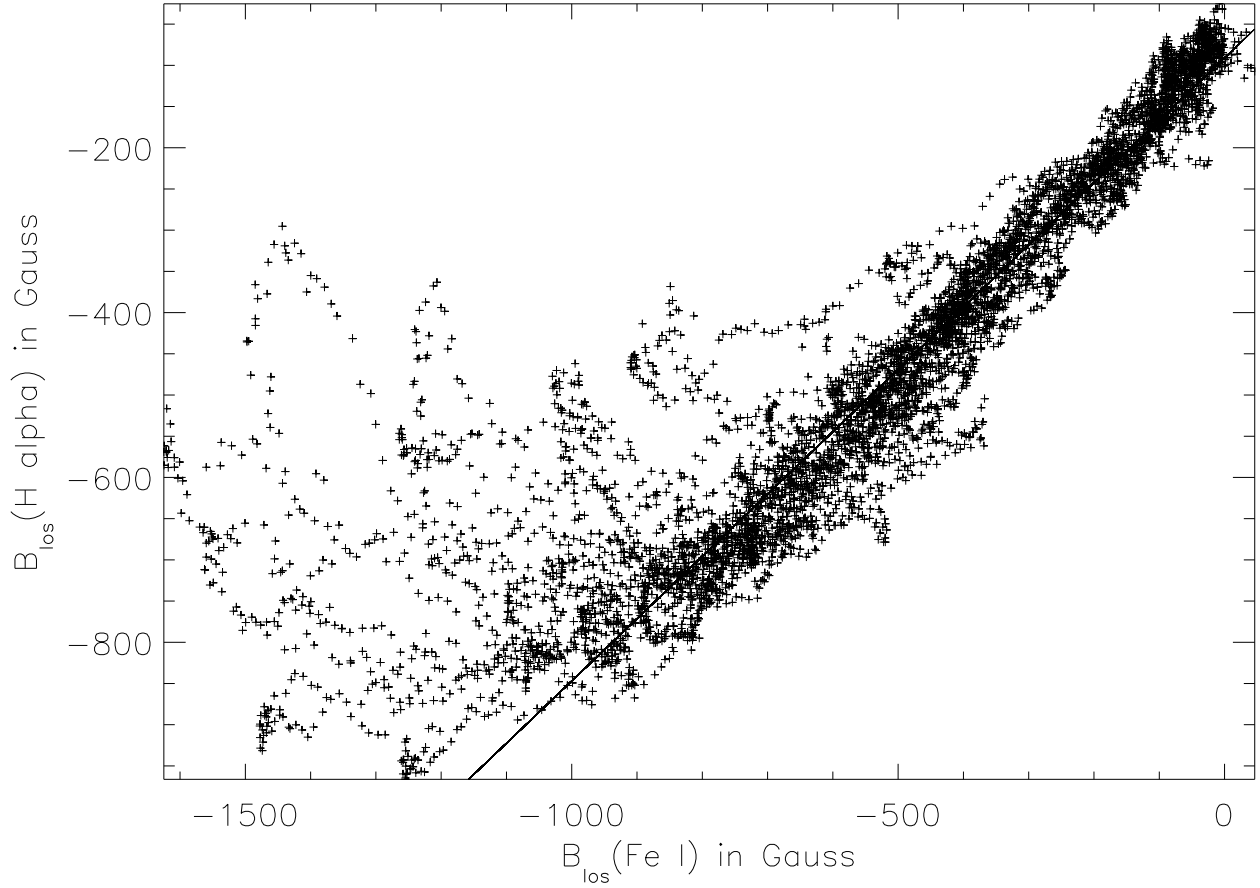


Fig. 2.— Scatter plot of photospheric and chromospheric LOS magnetic field derived using COG method applied to Fe I( $\lambda$ 6569) and  $H_{\alpha}$  respectively. Solid line is a linear fit to the field strengths correspond to the penumbral region.

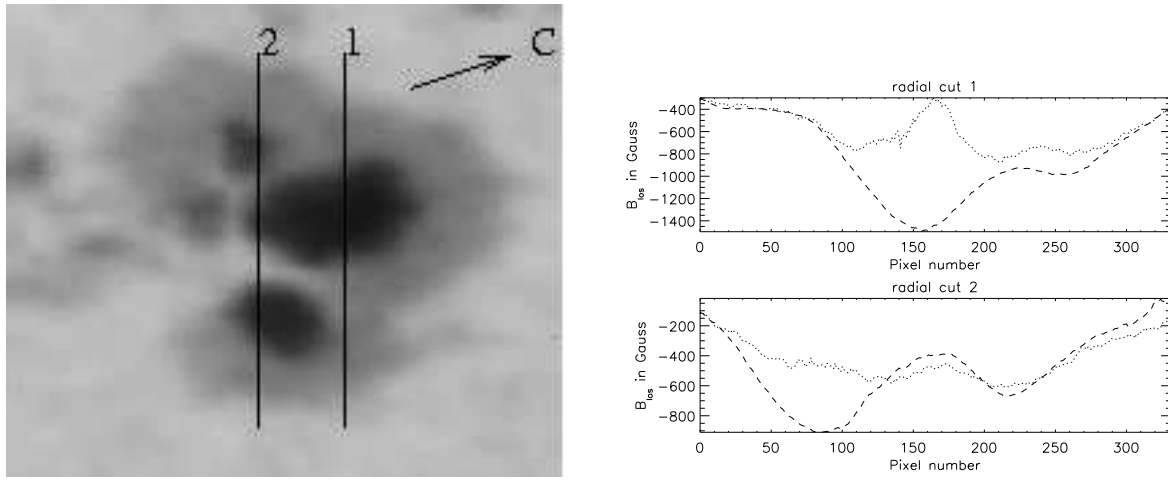


Fig. 3.— On the right side of this figure shown are the plots of LOS magnetic field strengths at the photosphere (dashed lines) and the chromosphere (dotted lines) along two radial slices of the sunspot. For reference, these two radial cuts are marked on the SOHO/MDI intensitygram. The arrow on the sunspot image indicates the disk center direction.

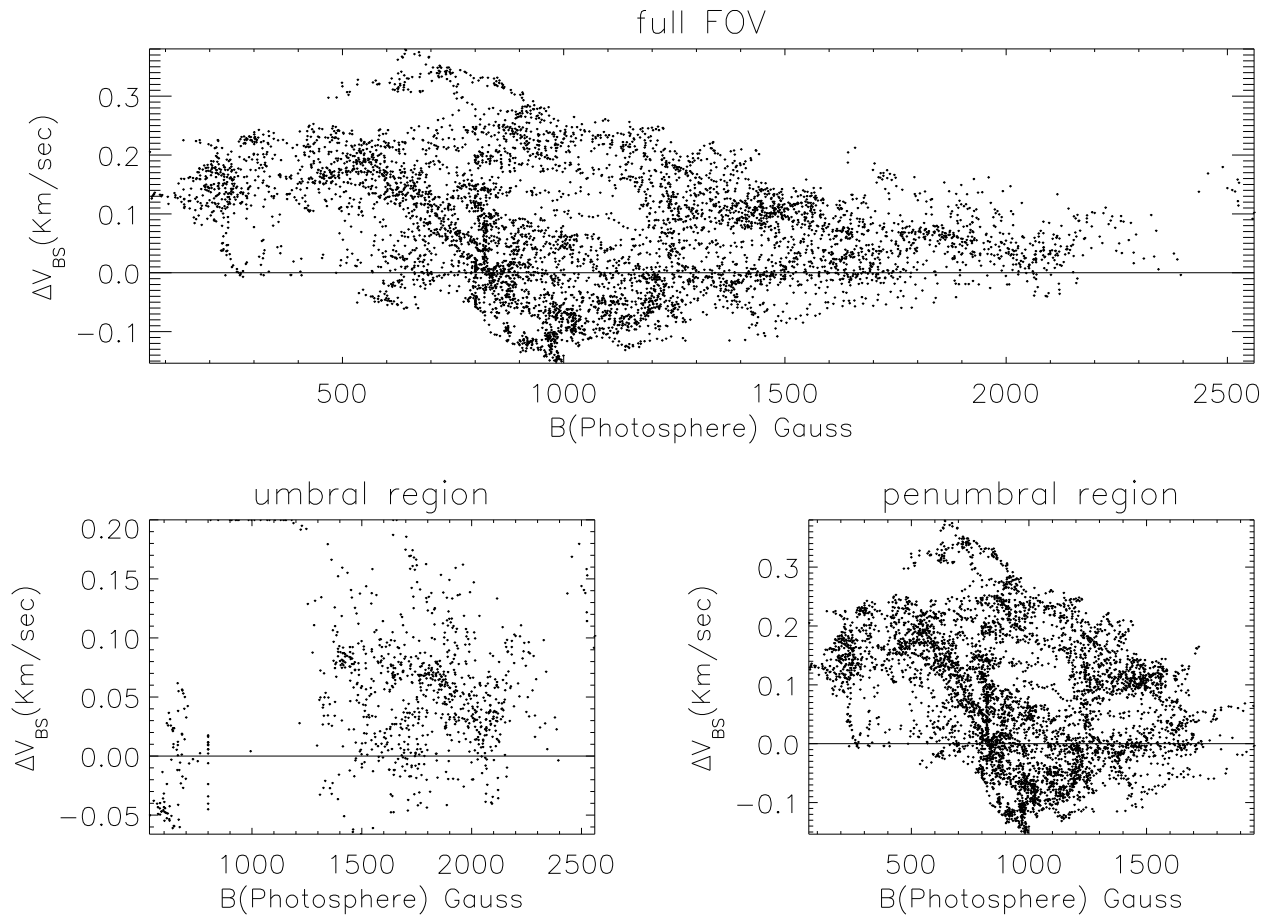


Fig. 4.— Plots of velocity gradients at the photosphere v/s photospheric magnetic field strength.

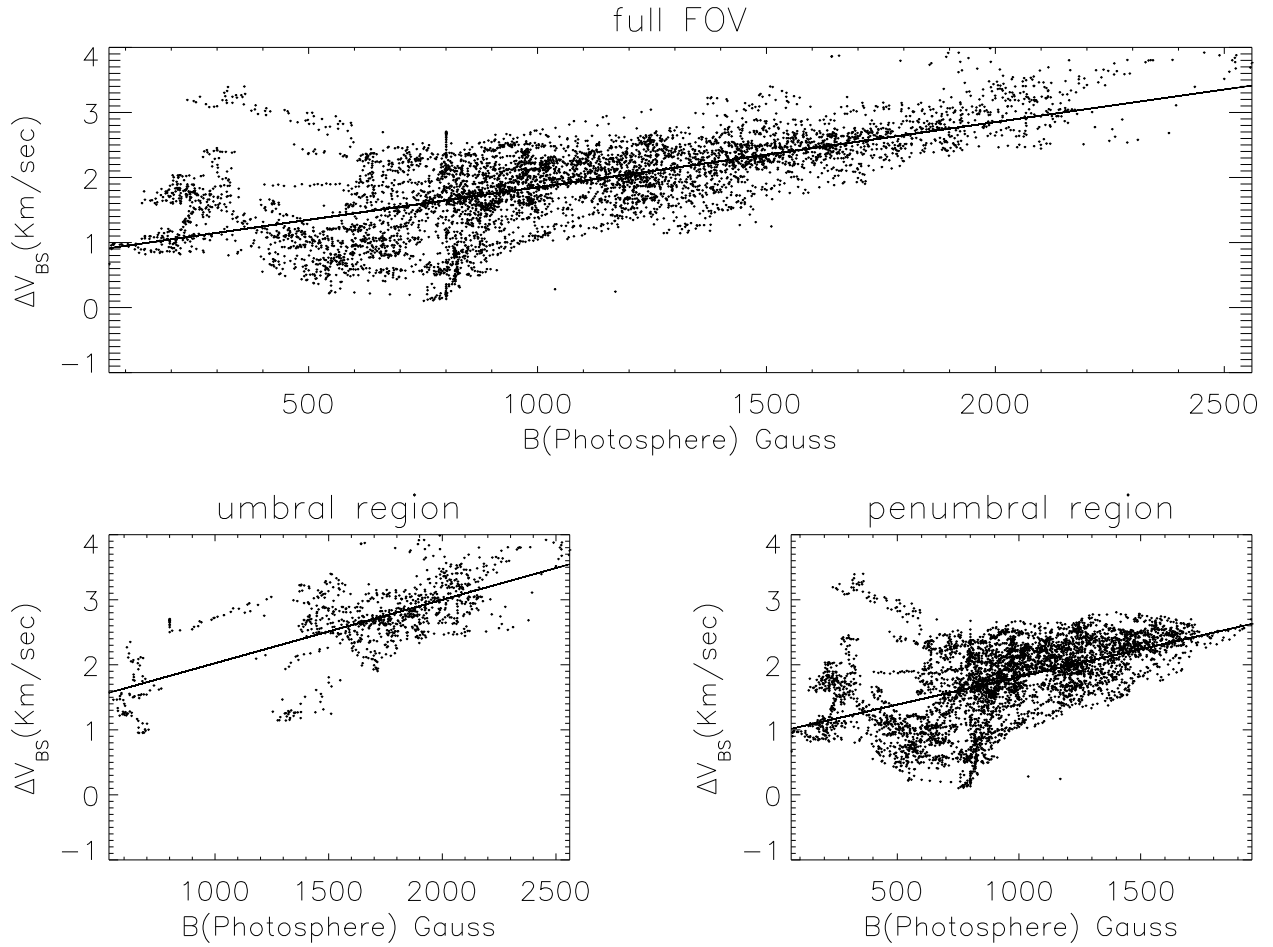


Fig. 5.— Plots of velocity gradients at chromosphere derived using  $H_\alpha$  with the bisectors considered for the full line profile v/s the total field strength (photospheric). Solid lines are the linear fit to the data points.

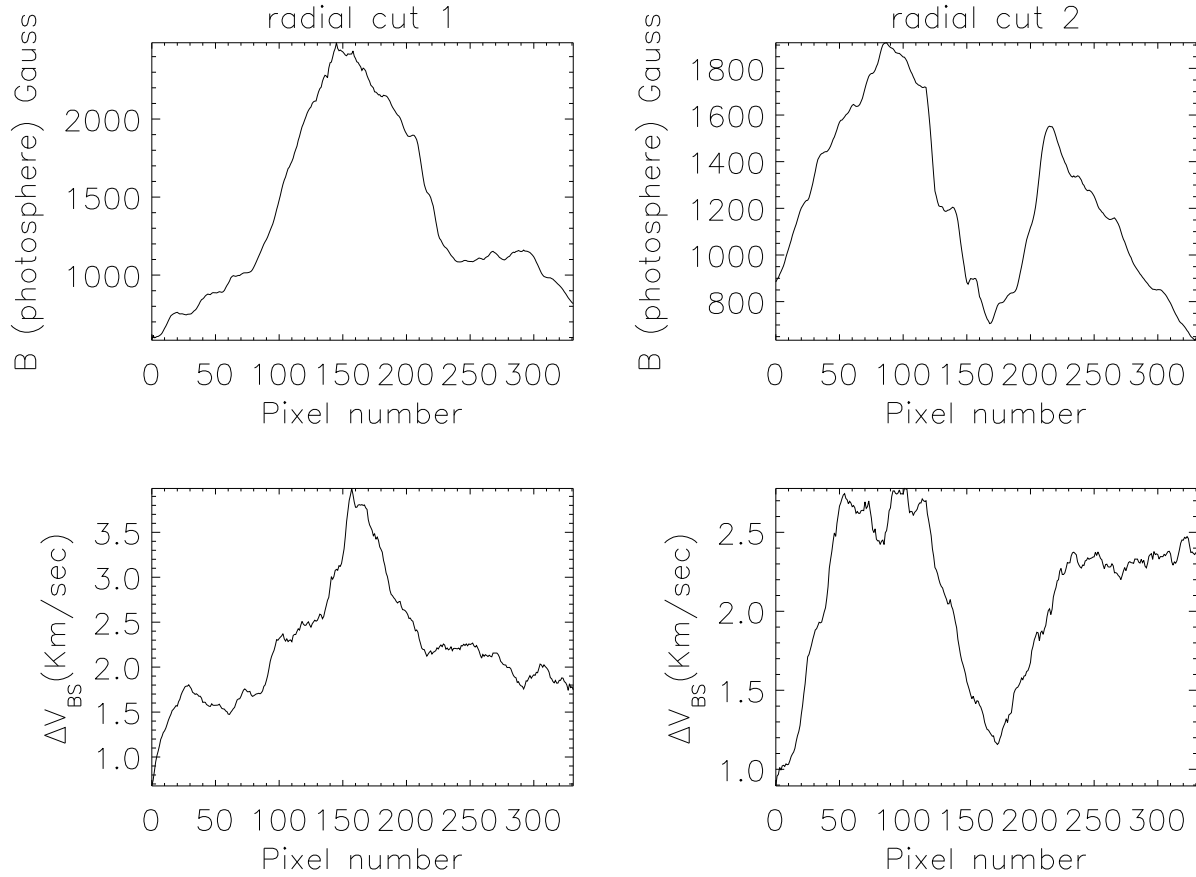


Fig. 6.— The top panels in this figure show the plots of magnetic field strength at the photosphere along two radial slices of the sunspot. The radial slices are same as those shown in Fig. 3. The corresponding plots of velocity gradients at the chromosphere are shown in the bottom panels.

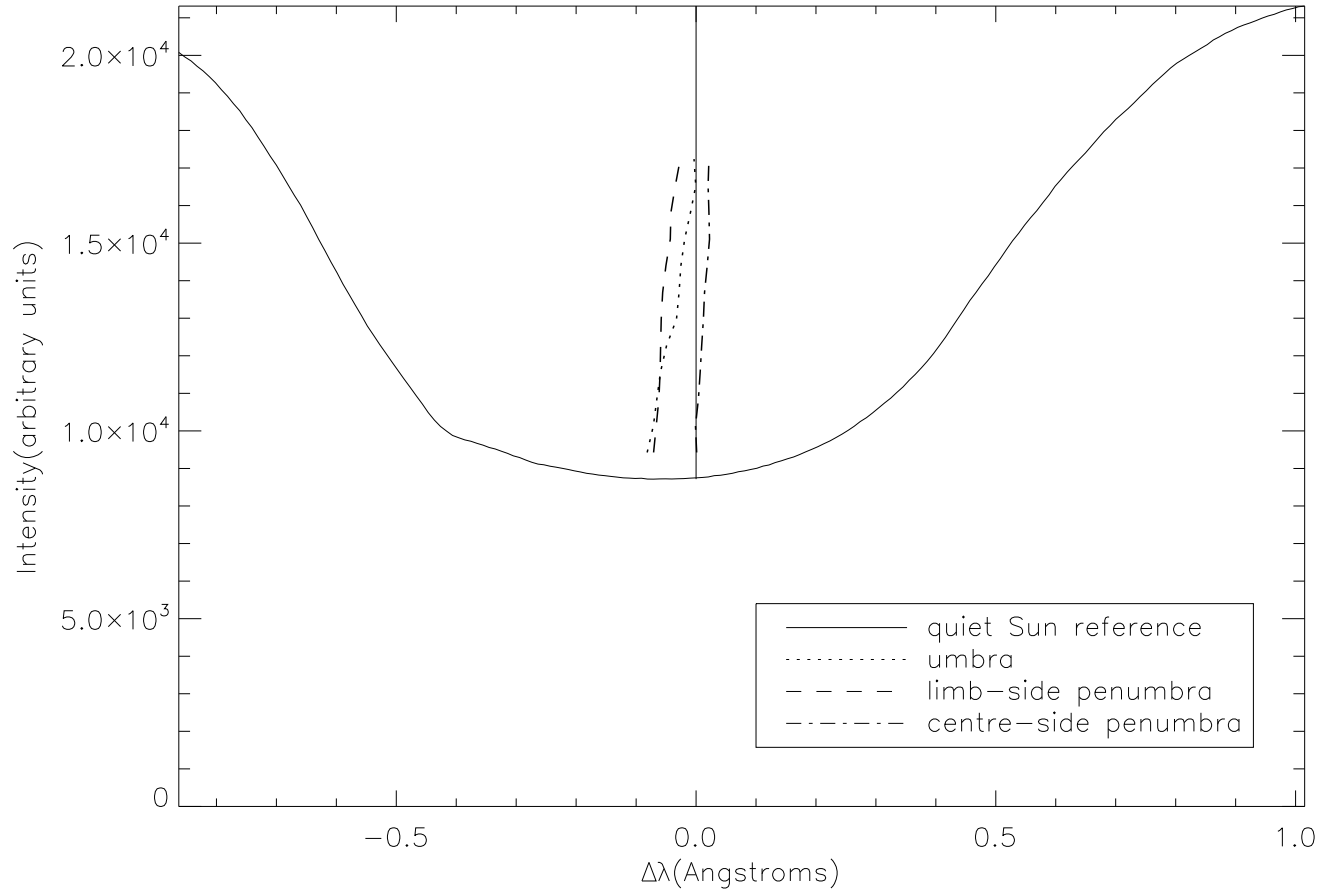


Fig. 7.— Representative bisectors of  $H_\alpha$  line profiles correspond to different regions of the sunspot are plotted on an average quiet Sun profile. The solid line represents the reference wavelength (which is a COG wavelength position of the nearby average quiet Sun profile). Dotted line represents the bisectors location typical of umbral profiles, dashed line-limb side penumbra, dash dotted line-center side penumbra.

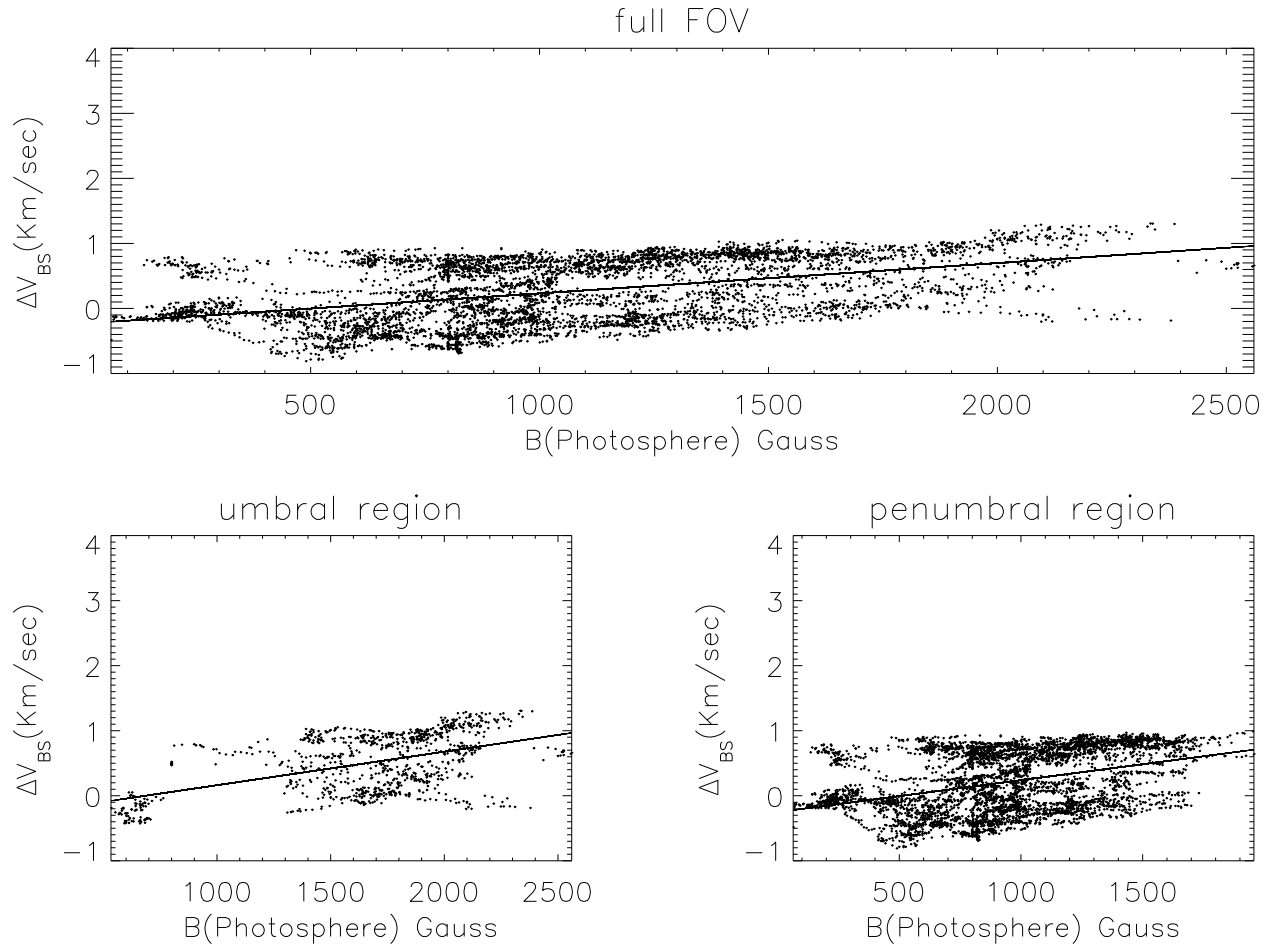


Fig. 8.— Same as Fig. 5 but with the limited spectral range about the line core considered for calculating velocity gradients to avoid the influence of blending due to Co I line. The axes scales are kept same as Fig. 5 to indicate that the velocity gradients are smaller compared to the case when the full Stokes  $I$  profile is considered.

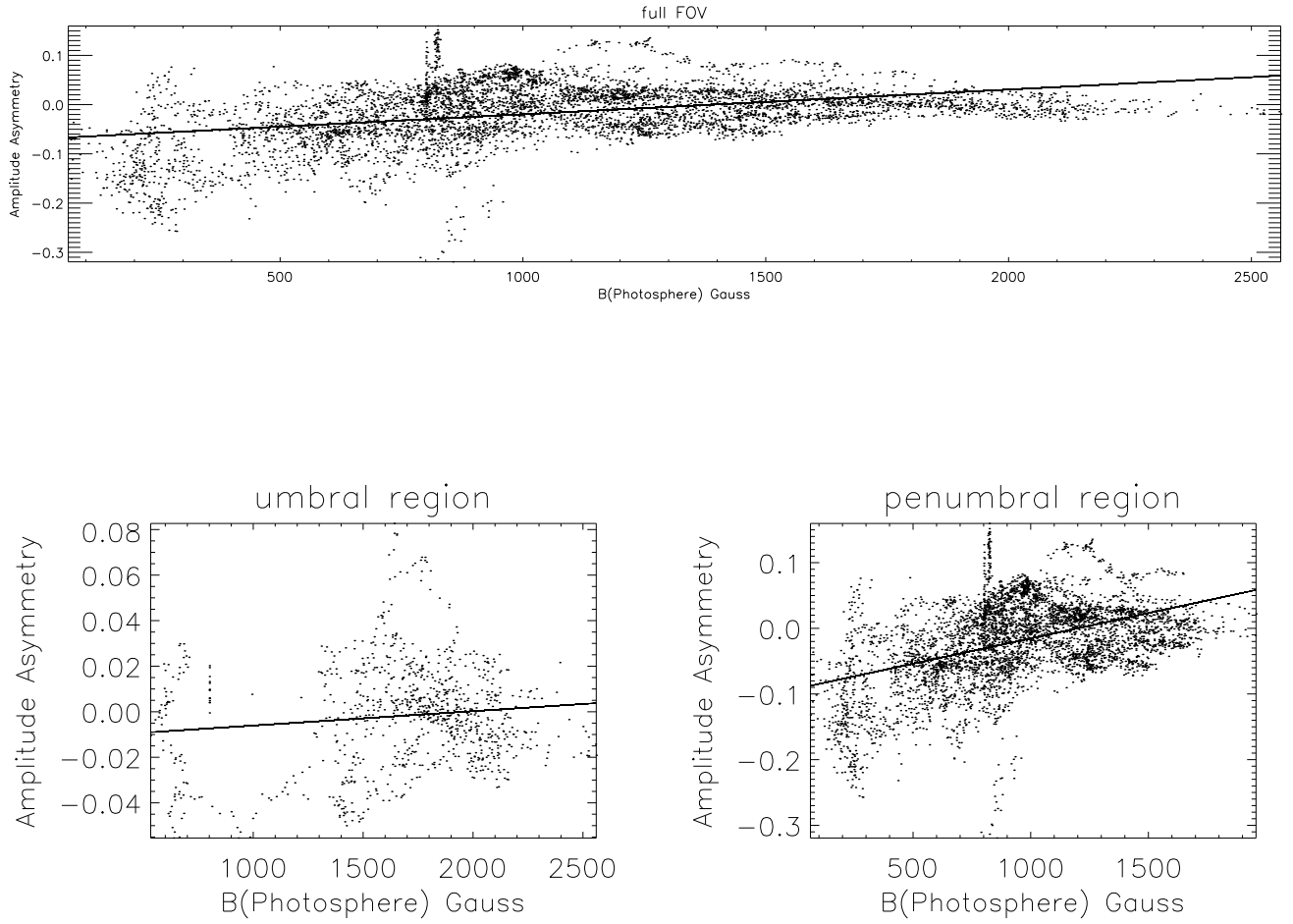


Fig. 9.— Plots of amplitude asymmetry of Stokes V profiles of Fe I line v/s the total field strength (photospheric). The solid lines are the linear fits to the data points.

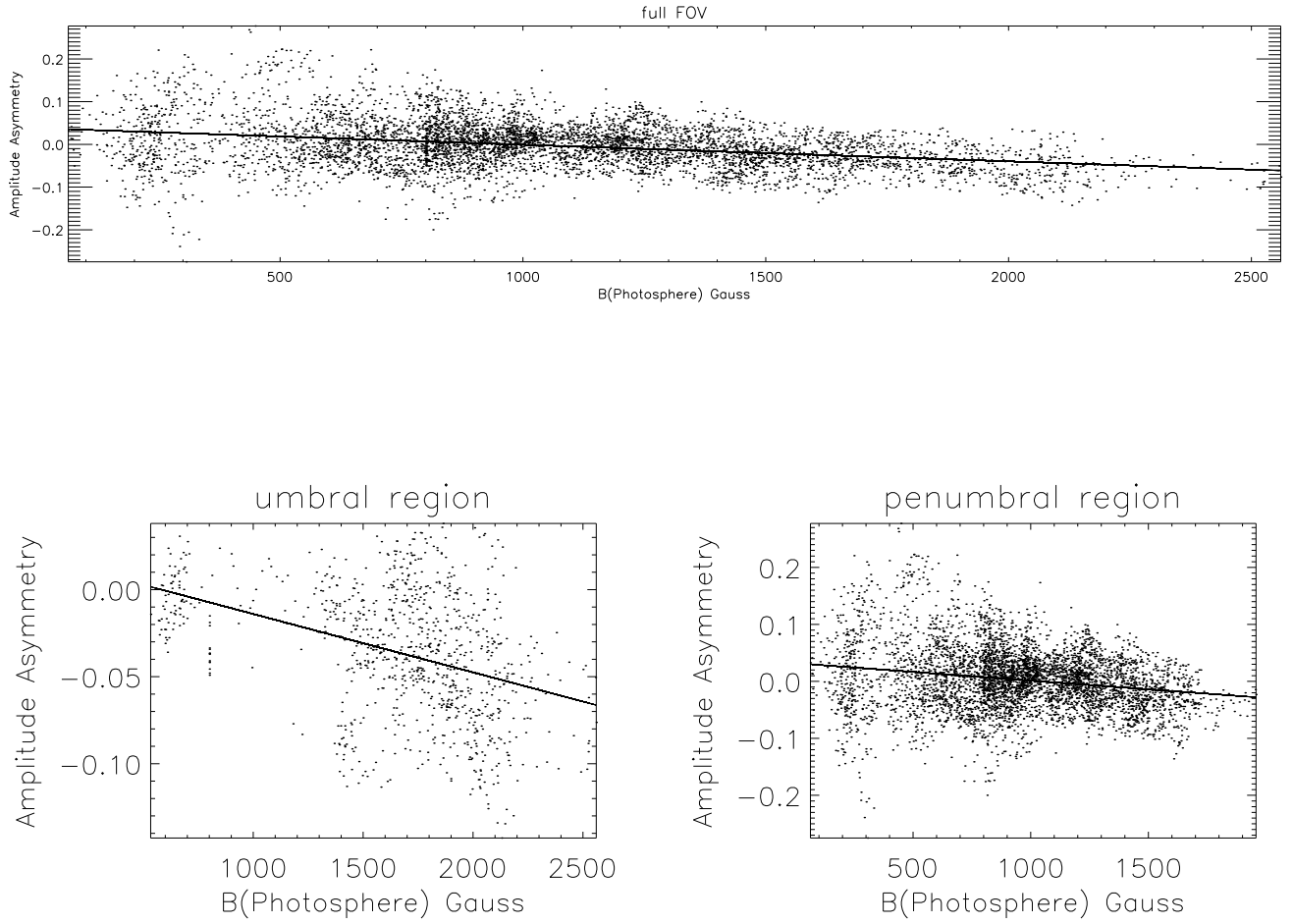


Fig. 10.— Plots of amplitude asymmetry of Stokes V profiles of  $H_{\alpha}$  line v/s the total field strength (photospheric). The solid lines are the linear fits to the data points.